Microscopic Structure and Elasticity of Weakly Aggregated Colloidal Gels

A. D. Dinsmore,[1] V. Prasad,[2,*] I. Y. Wong,[2,†] and D. A. Weitz[2]

[1]*Department of Physics, University of Massachusetts, Amherst, Massachusetts 01003, USA*

[2]*Department of Physics and Division of Engineering and Applied Sciences, Harvard University, Cambridge, Massachusetts 02138, USA*

(Received 24 October 2005; published 12 May 2006)

We directly probe the microscopic structure, connectivity, and elasticity of colloidal gels using confocal microscopy. We show that the gel is a random network of one-dimensional chains of particles. By measuring thermal fluctuations, we determine the effective spring constant between pairs of particles as a function of separation; this is in agreement with the theory for fractal chains. Long-range attractions between particles lead to freely rotating bonds, and the gel is stabilized by multiple connections among the chains. By contrast, short-range attractions lead to bonds that resist bending, with dramatically suppressed formation of loops of particles.

DOI: 10.1103/PhysRevLett.96.185502 PACS numbers: 61.43.Hv, 82.70.Dd, 83.80.Kn

When colloidal particles have an attraction between them, they can gel and form an elastic solid. Provided the strength of this attractive interaction, $U_{\max}$, is sufficiently large, a gel can form at arbitrarily low initial volume fractions, ϕ [1–3]. The elastic modulus of the resultant gel depends sensitively on both the nature and strength of the interparticle interaction and on the topology and connectedness of the gel [4–8]. This elasticity makes colloidal gels fascinating materials; it also imbues them with important practical properties, as the gels can form elastic materials with minute quantities of solids and are able to withstand significant shear stresses while still flowing freely once they yield. The essential structure of these gels is understood, provided that their formation results from kinetic aggregation: They are fractal on length scales up to a correlation length, ξ, and homogeneous on larger length scales. Both ξ and the fractal dimension d_f depend on the details of the aggregation. The elasticity of the networks is inherently much more complex than the structure, but can also be understood within this general scaling picture: The elastic modulus is $G \sim \kappa(\xi)/\xi$, where $\kappa(\xi)$ is the spring constant of a cluster of length ξ. This estimate is again predicated on the assumption that the sample is homogeneous at length scales above ξ and fractal at shorter length scales. The spring constant is estimated by assuming that the cluster is dominated by a single chain; the fractal nature makes this chain somewhat tortuous, and it is assumed that its contour length, L, scales with its end-to-end length, $L \sim \xi^{d_b}$, where d_b is the bond, or chemical dimension, whose value is 1.2 ± 0.1 [9,10]. It is also generally assumed that the bonds between neighboring particles resist bending, and this is the dominant contribution to the chain's elasticity. As a result, $\kappa(\xi) \sim \kappa_0/(\xi^{d_b} r_\perp^2)$ [11], where $r_\perp$ is the radius of gyration of the chain perpendicular to the line joining the two ends and $r_\perp \propto \xi^{d_b}$ in fractal gels [9]. Recent measurements of *isolated* chains of particles with rigid bonds confirmed this scaling of $\kappa(\xi)$ [12]. Since $\xi \sim a\phi^{-1/(3-d_f)}$, where a is the particle radius, the resultant ϕ dependence of the elastic modulus of a gel is $G \sim \kappa_0 \phi^{(1+2d_b)/(3-d_f)}$. This scaling description is in good agreement with data for kinetically aggregated colloidal gels [5,13–15]. However, this agreement is restricted to the ϕ dependence of G; a more critical test of the underlying physics would require visualization of gel topology and measurement of the scaling of the spring constant within the clusters at length scales less than ξ. Because of the difficulty of measuring both topology and local elasticity of a colloidal gel, such a test has never been performed.

In this Letter, we present real-space, three-dimensional images of colloidal gels that provide a direct probe of the detailed topology of a colloidal gel; we complement this with a measure of the scaling of the local spring constant determined by the thermal fluctuations of the network, directly observed with the confocal microscope. The attractive interaction that leads to gelation is induced by depletion, allowing us to vary the range of the attraction. We find unexpected dependence on this range: For a very short-ranged potential, the physical picture of the topology of the gel is in good accord with expectations, and the scaling model for the elasticity provides excellent agreement with the data. However, for a longer-range potential (but still $<2\%$ of the sphere diameter), the expected centrosymmetric behavior of the depletion interaction seems to apply; this leads to a dramatically different morphology of the network and different scaling of the elastic modulus with length. These measurements provide new, critical insight into the properties of colloidal gels and the essential relationship between their topology and their elasticity.

Our gels are made from monodisperse, sterically stabilized poly(methyl methacrylate) spheres [16] of radius $a = 0.75$ μm and with $\phi = 0.03$ to 0.05. They are suspended in a mixture of organic solvents chosen to match closely the particle density and refractive index [9,17,18], eliminating effects of sedimentation and allowing optical visualization deep within the sample. Particles are labeled with fluorescent rhodamine for observation with confocal microscopy [17]. The depletion attraction [19–22] is induced through

the addition of nonadsorbing polystyrene with molecular weights, M_w, of 9.6×10^4, 1.95×10^6, or 11.6×10^6 g/mol, corresponding to polymer radii, R_p, of approximately 6, 25, and 35 nm. The range of the depletion attraction is approximately $2R_p$, and its magnitude is estimated with the Asakura-Oosawa model, $U_d(r) = -\Pi_p V_{\text{overlap}}$, where $V_{\text{overlap}} = (R_p + a - r/2)^2(R_p + a + r/4)$ and r is the separation between sphere centers [19]. Because the polymer is in a good solvent, its R_p depends on concentration; we measure the size with static light scattering and determine the osmotic pressure by integrating the compressibility measured using static light scattering. The particles also have a weak repulsive interaction arising from electrostatic charge [23].

Confocal microscopy and image analysis are used to measure positions of each particle in the gel. Three-dimensional images of regions $40 \times 40 \times 30$ μm are acquired in approximately 5–10 s. Uncertainties in the centroid positions are approximately 0.05 μm in the three-dimensional images [17]. All images are taken at least 20 μm from the wall of the sample cell. Particles are considered to be bonded if their center-center separation falls below a cutoff value slightly larger than $2(a + R_p)$ [9]. The results are not sensitive to small variations in the cutoff length.

Both topological and structural information can be determined from 3D images. A false-color reconstruction of a typical image of a gel with $\phi = 0.04$ is shown in Fig. 1. For comparison, a two-dimensional image of the same sample after aging for 690 h is shown in the inset. This sample had $R_p = 25$ nm, corresponding to $R_p/a = 0.03$, and the polymer concentration was $c_p^{\text{eff}} = 7.2$ mg/ml, where c_p^{eff} is calculated using the volume accessible to the polymer, $V(1 - \phi)$. If the attraction were due solely to depletion, this would correspond to $U = -16k_BT$. Gelation took ~50 h and further aging was small; these data were collected 60 days after the sample was first initialized by shaking. The radial distribution function $g(r)$ exhibits a power-law decay $g(r) \sim r^{d_f - 3}$ as shown in Fig. 2(a); this provides a direct measure of the fractal dimension, $d_f = 2.1 \pm 0.1$. This value of d_f is consistent with that expected for irreversible reaction-limited cluster-cluster aggregation, which occurs when there is an energy barrier in the interaction potential between the particles that is overcome only rarely [24–29]. The expected correlation length is $a\phi^{-1/(3-d_f)} = 27 \pm 10$ μm. The images indicate that the gel is a network of intersecting chains. To identify individual chains between any two particles, we determine the contour length L of the shortest path between the particles *along the gel* [Fig. 3(a)] [9,10,30]. We measure the number of particles N in the chain connecting particles α and β by counting the number of particles γ that satisfy $L^{\alpha\gamma} + L^{\gamma\beta} \leq L^{\alpha\beta} + 1$ [9]. This definition selects all particles along the chain, as well as those attached to the side of the chain; these can strengthen or stiffen the network, as shown, for example, by the dark gray (blue) color in Fig. 1. We find that both L and N scale as r^{d_b}, with $d_b = 1.2 \pm 0.1$.

Although the gel is composed of chains of particles, it is nonetheless an interconnected structure where additional chains form loops, which can also connect particles. To ascertain their role in the gel's elasticity, we identify loops by searching for the next shortest path between two particles that does *not overlap* with the shortest path, except at the end points. An example is shown by the medium gray (red) particles in Fig. 1. The fraction of particle pairs for which a second path could be found, f_2, decreases rapidly with L as shown in Fig. 2(b). In all samples, the second-shortest paths are either rarely found ($f_2 \ll 1$) or they are very long ($\gg L$); this suggests that the local elasticity of the network is dominated by the shortest chain between any two particles.

The spring constant for each chain is directly measured from the thermal motion of the particles. We measure the distribution of separations, r, between two particles in

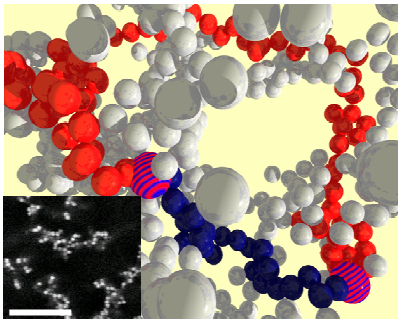

FIG. 1 (color online). Three-dimensional image of a colloidal gel reconstructed from confocal microscopy. The dark gray (blue) particles form the shortest chain connecting the two particles α and β (enlarged, in stripes). The second-shortest path is shown in medium gray (red). Inset: Raw image of a slice through the same gel. The scale bar is 20 μm.

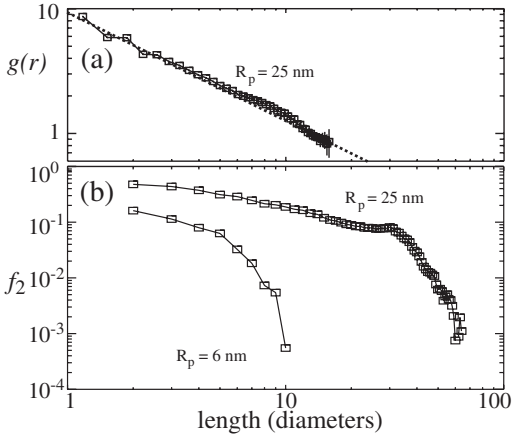

FIG. 2. (a) Pair distribution function g vs separation r. The dotted line corresponds to a fractal dimension, $d_f = 2.1$. (b) Probability of finding a second path between two particles, f_2, as a function of their shortest-path length, L.

several hundreds to thousands of images, and assume that its probability distribution is determined by the Boltzmann factor, $P(r) \sim \exp\{-U(r)/k_BT\}$. When averaged over several pairs of particles with similar r, $U(r)$ is well described by a parabola as shown in Fig. 3(a). The curvature provides a direct measure of the average elastic constant, $\kappa(r)$, of the chain connecting two particles with mean separation r. We also determine the spring constants of *individual* chains using the equipartition theorem, which gives $\kappa = k_BT(\langle r^2\rangle - \langle r\rangle^2)$. This method of analysis corresponds to integrating out the motions of the springs that act in parallel. Explicit calculations suggest that this approximation is accurate to within a few percent because the other springs are much longer and hence weaker than the principal chain. In all cases, we account for the uncertainty in particle position, which can be significant for small r.

Measurements of the spring constant allow us to determine its scaling with length. We measure the length dependence in terms of N and show a scatter plot of all 3036 measured single-chain values in Fig. 3(b); the large squares represent the mean values of κ for all chains with a given value of N. Surprisingly, we find $\kappa \propto N^{-1}$ and hence $\kappa \propto r^{-d_b}$; this differs from the scaling expected for diffusion-limited cluster aggregation. In the inset, we plot $N\kappa(r)$ as a function of $r_\perp^2$, explicitly confirming that $\kappa(r)$ is independent of $r_\perp^2$. We also measure the distribution of spring constants for each value of r and find this to be independent of the chain length; thus not only the average value κ exhibits this scaling, but all moments of κ do as well. Furthermore, similar behavior was observed for this sample when measured after 4, 13, 20, and 29 days; similar behavior was also observed for a separate sample with $c_p^{\text{eff}} = 8.9$ mg/ml. Similar behavior is also found for gels with still longer-range attraction, formed using polymer with $R_p = 33$ and 35 nm. Thus, this is a very robust result. The spring constant has the N^{-1} scaling that is characteristic of one-dimensional chains that resist stretching but not bending, as would be expected for a centrosymmetric potential such as depletion.

We find a striking difference in the r dependence of $\kappa(r)$ for chains in samples with shorter-ranged interactions. We measure the structure and elastic constants of a sample with $\phi = 0.04$ and $R_p = 6$ nm, corresponding to $R_p/a = 0.008$ and $c_p^{\text{eff}} = 22.3$ mg/ml. Although this sample is assumed to be a fractal gel like the others, its topology differs significantly from that of samples with longer-ranged potentials: there are significantly fewer loops, as shown by the f_2 data in Fig. 2(b). In general, such a topological difference is not apparent from $g(r)$ and hence cannot be discerned by scattering. For this sample we find $\kappa(r) \sim (Lr_\perp^2)^{-1}$ at distances greater than several times a, as shown in Fig. 4. Here we explicitly calculate L and $r_\perp$ for each pair and show $(Lr_\perp^2)^{-1}$ with the solid line; it is in good agreement with the data. This behavior is consistent with the expectations for chains that resist bond bending, which is typically inferred from the elastic behavior of

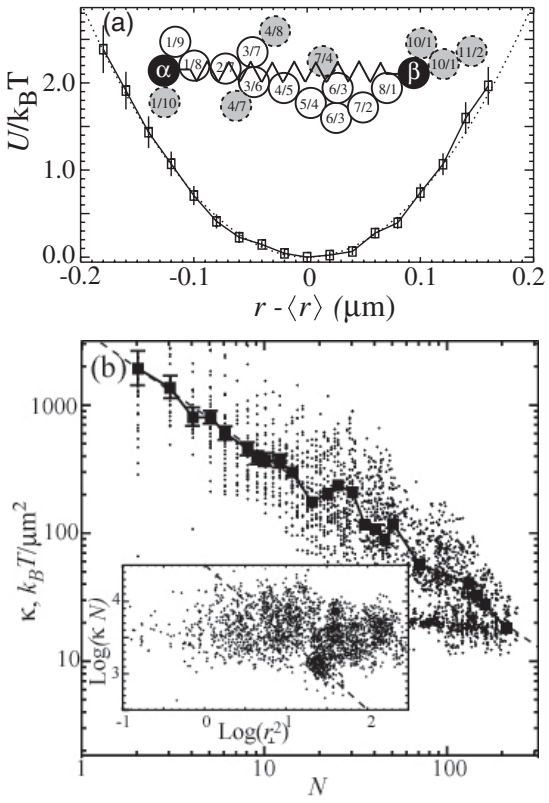

FIG. 3. (a) Plot of $U(r)$ measured for pairs of particles with $N = 18$ in a sample with long-ranged interaction ($R_p = 35$ nm); the dotted curve is a fit with elastic constant $\kappa = 146 \pm 6k_BT/\mu m^2$. Inset: Illustration of a chain with $L = 9$ and $N = 13$. The numbers show the lengths $L^{\alpha\gamma}/L^{\beta\gamma}$ of the shortest path between each particle (γ) and the particles α and β. (b) Scaling of spring constant, κ, with the number of particles in a chain, N, for a sample with medium-range depletion attraction ($R_p = 25$ nm, $\phi = 0.04$). The straight line represents $\kappa \propto 1/N$. Inset: Log-log plot of κN vs $r_\perp^2$. The dashed line shows a slope of -1, which is expected to apply for rigid chains.

kinetically aggregated colloids [5,6]. While depletion should be a centrosymmetric potential, the range of the potential here is so small that it is comparable to the length of the steric stabilization layer on the particles (≈10 nm [31]). We speculate that the attraction is sufficiently large to cause overlap of the stabilizing layers or meshing of surface asperities, resulting in a resistance to bond bending.

The spring constant has a different r dependence at both long and short r. At long length scales, the mean elastic constant becomes independent of chain length, as shown in Fig. 4 for $r > 20$ μm, which is close to the estimate of $\xi = 27$ μm. In this regime, the elasticity of the gel is dominated by the highly interconnected network of chains, so κ is nearly independent of length, as expected for an isotropic material [32]. By contrast, at the shortest r, we again observe $\kappa(r) \sim N^{-1}$, similar to the longer-ranged potential; at these length scales, bond-stretching elasticity is weaker than that of bond bending.

We estimate the spring constant κ_s for stretching the bond between two neighboring particles from the interac-

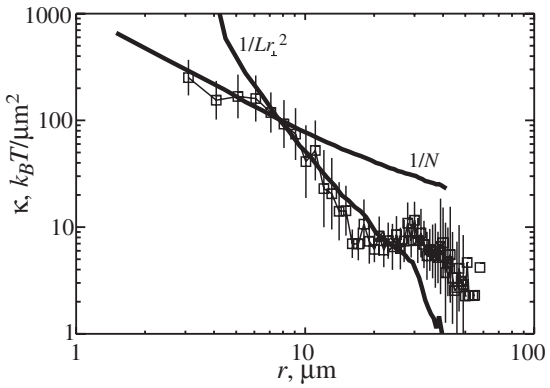

FIG. 4. Log-scale plot of the mean κ vs Euclidean separation, r (squares), for a sample with short-range depletion attraction ($R_p = 6$ nm). Also plotted are $1585/\langle N\rangle$ and $3162/\langle Lr_\perp^2\rangle$; the numerical coefficients were chosen to overlay the data with $\kappa(r)$.

tion potential. This potential includes both the depletion attraction and the electrostatic repulsion. The latter can be roughly estimated from the gelation time by assuming that the increase over that expected from purely diffusion-limited cluster aggregation reflects the contribution of an electrostatic repulsive barrier [33]. We then predict the bond-stretching spring constant κ_s by calculating the mean-square fluctuation in separation between two particles; this is similar to the way $\kappa(r)$ is determined in our experiments. We compare this estimate to the contact value, κ_0, determined experimentally by extrapolating our data to $r = 2a$. For the shortest-range potential, the predicted κ_s is 3–4 orders of magnitude greater than that measured, consistent with bond bending being dominant. By contrast, for the longer-range potentials the predicted κ_s are 1–2 orders of magnitude greater than those measured [28].

The network formed with the shortest-ranged potential exhibits behavior consistent with that expected for kinetically aggregated fractal gels; the elasticity is determined by bond bending and exhibits the predicted scaling at lengths shorter than the correlation length [11]. By contrast, it is striking that the gels formed with a longer-ranged potential remain stable despite the fact that the bonds do not resist bending. An isolated chain would collapse into a dense, rigid aggregate. By contrast, in the gel each chain is linked to other chains at several points, resulting in a relatively larger number of loops. These links are quite dense; we observe no isolated chainlike sequences of particles with only two bonds per particle [9]. Thus the bond-bending degree of freedom must lead to formation of many loops during the gelation. These multiple links or loops maintain the shape of the chains and suppress bond rotation. This suggests that the network is not in equilibrium and would shrink if it were not attached to the walls. These results highlight the unusual structures formed by randomly aggregated colloids.

We thank Eric Weeks, Barbara Frisken, Jean-Pierre Bouchaud, Erwin Frey, Robin Ball, and Yakov Kantor for valuable discussions. I. Y. W. is grateful for support from the Harvard College Research Program. This work was supported by the NSF (DMR-0243715) and NASA (NAG3-2284).

*Present address: Department of Physics, Emory University, Atlanta, GA 30322, USA.
†Present address: Stanford University, Department of Materials Science, Palo Alto, CA 94305, USA.

[1] M. Carpineti and M. Giglio, Phys. Rev. Lett. **68**, 3327 (1992).
[2] D. Asnaghi, M. Carpineti, and M. Giglio, MRS Bull. **19**, 14 (1994).
[3] S. Manley *et al.*, Phys. Rev. Lett. **93**, 108302 (2004).
[4] P. Patel and W. Russel, J. Colloid Interface Sci. **131**, 192 (1989).
[5] M. C. Grant and W. B. Russel, Phys. Rev. E **47**, 2606 (1993).
[6] A. H. Krall and D. A. Weitz, Phys. Rev. Lett. **80**, 778 (1998).
[7] S. Ikeda, E. A. Foegeding, and T. Hagiwara, Langmuir **15**, 8584 (1999).
[8] V. Prasad *et al.*, Faraday Discuss. **123**, 1 (2003).
[9] A. D. Dinsmore and D. A. Weitz, J. Phys. Condens. Matter **14**, 7581 (2002).
[10] P. Meakin *et al.*, J. Phys. A **17**, L975 (1984).
[11] Y. Kantor and I. Webman, Phys. Rev. Lett. **52**, 1891 (1984).
[12] J. P. Pantina and E. M. Furst, Phys. Rev. Lett. **94**, 138301 (2005).
[13] W.-H. Shih *et al.*, Phys. Rev. A **42**, 4772 (1990).
[14] A. A. Potanin *et al.*, J. Chem. Phys. **102**, 5845 (1995).
[15] W. Wolthers *et al.*, Phys. Rev. E **56**, 5726 (1997).
[16] L. Antl *et al.*, Colloids Surf. **17**, 67 (1986).
[17] A. D. Dinsmore *et al.*, Appl. Opt. **40**, 4152 (2001).
[18] E. R. Weeks *et al.*, Science **287**, 627 (2000).
[19] S. Asakura and F. Oosawa, J. Polym. Sci. **33**, 183 (1958).
[20] W. C. K. Poon, Curr. Opin. Colloid Interface Sci. **3**, 593 (1998).
[21] S. M. Ilett *et al.*, Phys. Rev. E **51**, 1344 (1995).
[22] A. D. Dinsmore, A. G. Yodh, and D. J. Pine, Phys. Rev. E **52**, 4045 (1995).
[23] M. F. Hsu, E. R. Dufresne, and D. A. Weitz, Langmuir **21**, 4881 (2005).
[24] M. Kolb, Phys. Rev. Lett. **53**, 1653 (1984).
[25] D. A. Weitz *et al.*, Phys. Rev. Lett. **54**, 1416 (1985).
[26] P. Meakin and F. Family, Phys. Rev. A **38**, 2110 (1988).
[27] W. Y. Shih *et al.*, J. Stat. Phys. **62**, 961 (1991).
[28] M. D. Haw *et al.*, Adv. Colloid Interface Sci. **62**, 1 (1995).
[29] J. L. Burns *et al.*, Colloids Surfaces A: Physicochem. Eng. **162**, 265 (2000).
[30] S. Havlin and R. Nossal, J. Phys. A **17**, L427 (1984).
[31] S. E. Phan *et al.*, Phys. Rev. E **54**, 6633 (1996).
[32] A. M. Kosevich *et al.*, *Theory of Elasticity* (Butterworth-Heinemann, Oxford, 1986).
[33] See EPAPS Document No. E-PRLTAO-96-042621 for estimates of spring constants from the interparticle potentials. For more information on EPAPS, see http://www.aip.org/pubservs/epaps.html.